

## Supporting Information

### **Cyclic graft copolymer unimolecular micelles: Effects of cyclization on particle morphology and thermoresponsive behavior**

Rebecca J. Williams, Anaïs Pitto-Barry, Nigel Kirby, Andrew P. Dove\* and

Rachel K. O'Reilly\*

#### Contents

Materials .....	2
General Considerations .....	2
Experimental Procedures .....	5
General procedure for ring-opening polymerizations .....	5
General procedure for alkyne end-group functionalization .....	5
Synthesis of bis-(azidoethyl)disulfide ( <b>3</b> ) .....	6
General procedure for cyclization via the copper-catalyzed azide-alkyne cycloaddition .....	7
General procedure for RAFT polymerizations .....	8
Characterization Data.....	8

## Materials

1,8-Diazabicyclo[5.4.0]undec-7-ene (DBU) was dried over  $\text{CaH}_2$ , distilled and stored under inert atmosphere. 1,4-butanediol was dried and stored over 3 Å molecular sieves. Monomer **1** was prepared according to our previously reported method and dried over 3 Å molecular sieves in dry  $\text{CH}_2\text{Cl}_2$ .<sup>1</sup> 5-Methyl-5-ethoxycarbonyl-1,3-dioxan-2-one (**2**) was synthesized as reported and dried over 3 Å molecular sieves in dry  $\text{CH}_2\text{Cl}_2$ .<sup>2</sup> 4-Pentynoic anhydride was prepared according to the literature.<sup>3</sup> AIBN (2,2'-azo-bis(isobutyronitrile)) was recrystallized twice from methanol and stored in the dark below 4 °C.  $\text{CH}_2\text{Cl}_2$  was purified over Innovative Technology SPS alumina solvent columns and degassed before use. Nanopure water with a resistivity of 18 MΩ·cm was prepared using a Millipore Simplicity UV ultrapure water purification system. All other solvents and chemicals were obtained from Sigma-Aldrich or Fisher Scientific and used as received.

## General Considerations

Ring-opening polymerizations were performed under inert atmosphere in a glovebox. RAFT polymerizations were carried out under oxygen-free conditions using standard Schlenk-line techniques.  $^1\text{H}$  and  $^{13}\text{C}$  NMR spectra were recorded on a Bruker DPX-300, DPX-400 or AC-400 spectrometer at 298 K. Chemical shifts are reported as  $\delta$  in parts per million (ppm) and referenced to the chemical shift of the residual solvent resonances ( $\text{CHCl}_3$ :  $^1\text{H}$   $\delta$  = 7.26 ppm;  $^{13}\text{C}$   $\delta$  = 77.16 ppm,  $\text{H}_2\text{O}$ :  $^1\text{H}$   $\delta$  = 4.79 ppm). IR spectra were recorded using a Perkin-Elmer Spectrum 100 FT-IR spectrometer. Spectra were an accumulation of 16 scans with the background subtracted. UV-Vis spectra were recorded using a Perkin-Elmer UV-Vis Spectrometer (Lambda 35). Size exclusion chromatography (SEC) analysis in  $\text{CHCl}_3$  was conducted on a Varian Polymer Laboratories PL-GPC 50 plus integrated SEC system with differential refractive index and ultraviolet detectors equipped with a guard column (Varian

Polymer Laboratories PLGel 5  $\mu\text{M}$ ,  $50 \times 7.5$  mm) and two mixed D columns (Varian Polymer Laboratories PLGel 5  $\mu\text{M}$ ,  $300 \times 7.5$  mm). The mobile phase was  $\text{CHCl}_3$  with 0.5% triethylamine at a flow rate of  $1.0 \text{ mL min}^{-1}$ . SEC samples were calibrated against Varian Polymer Laboratories Easi-Vials linear poly(styrene) standards ( $162 - 2.4 \times 10^5 \text{ g mol}^{-1}$ ) or Varian Polymer Laboratories Easi-Vials linear poly(methyl methacrylate) standards ( $690 - 1.9 \times 10^6 \text{ g mol}^{-1}$ ) using Cirrus v3.3 software. MALDI-ToF (matrix-assisted laser desorption ionization time of flight) spectra were recorded using a Bruker Daltronics Ultraflex II MALDI-ToF mass spectrometer, equipped with a nitrogen laser delivering 2 ns laser pulses at 337 nm with a positive ion ToF detection performed using an accelerating voltage of 25 kV. Samples were spotted onto a Bruker ground steel MALDI-ToF analytical plate through application of a small portion of a solution containing trans-2-[3-(4-*tert*-butylphenyl)-2-methyl-2-propylidene]malonitrile (DCTB) as a matrix (20  $\mu\text{L}$  of a  $10 \text{ mg mL}^{-1}$  solution in THF), sodium trifluoroacetate as a cationization agent (5  $\mu\text{L}$  of a  $10 \text{ mg mL}^{-1}$  solution in THF), and analyte (5  $\mu\text{L}$  of a  $10 \text{ mg mL}^{-1}$  solution in THF) followed by solvent evaporation. The samples were measured in linear or reflectron ion mode and calibrated by comparison to  $2 \times 10^3$  poly(ethylene oxide) standards. Cryogenic TEM was performed using a JEOL 2010F TEM operated at 200 kV and imaged using a Gatan Ultrascan 4000 camera. Dynamic light scattering (DLS) measurements were taken on a Malvern Zetasizer NanoS instrument with a 4 mW He-Ne 633 nm laser module and the data analyzed using Malvern DTS v7.3.0 software. Measurements were taken at a detection angle of  $173^\circ$ . The hydrodynamic diameter ( $D_h$ ) was calculated from the Stokes-Einstein equation  $D_h = kT/(3\pi\eta D_{\text{app}})$ , where  $k$  is the Boltzmann constant,  $T$  is the temperature,  $\eta$  is the viscosity of the solvent and  $D_{\text{app}}$  the apparent diffusion coefficient, where  $D_{\text{app}} = \Gamma/q^2$ .  $q$  is the scattering vector and  $q = (4\pi n/\lambda)\sin(\theta/2)$ , where  $\theta$  is the scattering angle,  $\lambda$  is the laser wavelength,  $n$  is the refractive index of the solvent and  $\Gamma$  is the relaxation rate of the scatters. The intensity-weighted size

distribution is derived from the Distribution analysis method and the volume- and number-weighted size distributions are derived from the intensity-weighted distribution using Mie theory.  $D_h$  only coincides with the real hydrodynamic diameter when the measured sample consists of monodisperse spherical particles. SAXS measurements were recorded at the Australian Synchrotron facility at a photon energy of 11 keV and a sample to detector distance of 3.252 m to give a  $q$  range of 0.004 to 0.2  $\text{\AA}^{-1}$ .  $q$  is the scattering vector and is related to the scattering angle ( $2\theta$ ) and the photon wavelength ( $\lambda$ ) by  $q = 4\pi\sin(\theta)/\lambda$ . The scattering from a blank ( $\text{H}_2\text{O}$  or 1,4-dioxane) was measured and subtracted for each measurement and data were normalized for total transmitted flux using a quantitative beamstop detector and absolute scaled using water as an absolute intensity standard. The two-dimensional SAXS images were converted into one-dimensional SAXS profiles ( $I(q)$  versus  $q$ ) by circular averaging. NCNR Data Analysis IGOR PRO software was used to plot and analyse SAXS data and the models used for form fitting were taken from the NCNR package. Scattering length densities (SLD) were calculated using the “Scattering Length Density Calculator” provided by the NIST Center for Neutron Research, using the equation  $\text{SLD} = \Sigma Zr_e/V_m$ , where  $V_m$  is molecular volume,  $Z$  is atomic number and  $r_e$  is electron radius. SLS experiments were performed at angles of observation ranging from  $30^\circ$  to  $150^\circ$  with an ALV CG3 spectrometer operating at  $\lambda_0 = 633$  nm and at  $20 \pm 1$   $^\circ\text{C}$ . Data were collected in duplicate with 30 s run times. Calibration was achieved with filtered toluene and the background was measured with filtered solvent (18.2  $\text{M}\Omega\cdot\text{cm}$  water). Lower critical solution temperature (LCST) measurements were recorded using a Perkin-Elmer UV-Vis Spectrometer (Lambda 35) equipped with a Peltier temperature controller at 500 nm with a heating/cooling rate of 1  $^\circ\text{C min}^{-1}$ . An average of three heating/cooling cycles were reported for each sample.

## Experimental Procedures

### *General procedure for ring-opening polymerizations*

1,8-Diazabicyclo[5.4.0]undec-7-ene (DBU) was added to a solution of the appropriate equivalents of **1**, **2** and 1,4-butanediol (taken from a stock solution of 1,4-butanediol in dry CH<sub>2</sub>Cl<sub>2</sub>) in dry CH<sub>2</sub>Cl<sub>2</sub> and stirred at room temperature. After the desired amount of time the polymerization was quenched by the addition of Amberlyst 15 H<sup>+</sup> ion exchange resin. The resin was removed by filtration and CH<sub>2</sub>Cl<sub>2</sub> removed under reduced pressure. The unreacted monomers and residual DBU were removed by column chromatography (silica, 100% CH<sub>2</sub>Cl<sub>2</sub>, then 100% ethyl acetate).

**P2:** <sup>1</sup>H NMR (400 MHz, CDCl<sub>3</sub>, ppm):  $\delta$  = 7.31 – 7.26 (m, 4H<sub>backbone-1</sub>, Ar), 5.11 (m, 2H<sub>backbone-1</sub>, OCH<sub>2</sub>Ar), 4.59 (m, 2H<sub>backbone-1</sub>, SCH<sub>2</sub>Ar), 4.28 (m, 8H<sub>backbone-1+2</sub>, C=OOCH<sub>2</sub>C(CH<sub>3</sub>)CH<sub>2</sub>O), 4.17 (m, 2H<sub>backbone-2</sub>, OCH<sub>2</sub>CH<sub>3</sub>), 4.11 (m, 4H<sub>end-group</sub>, OCH<sub>2</sub>CH<sub>2</sub>), 3.37 (m, 2H<sub>backbone-1</sub>, SCH<sub>2</sub>CH<sub>3</sub>), 1.73 (m, 4H<sub>end-group</sub>, OCH<sub>2</sub>CH<sub>2</sub>), 1.35 (m, 3H<sub>backbone-1</sub>, SCH<sub>2</sub>CH<sub>3</sub>), 1.24 (m, 6H<sub>backbone-1+2</sub>, CCH<sub>3</sub>), 1.21 (m, 3H<sub>backbone-2</sub>, OCH<sub>2</sub>CH<sub>3</sub>).

### *General procedure for alkyne end-group functionalization*

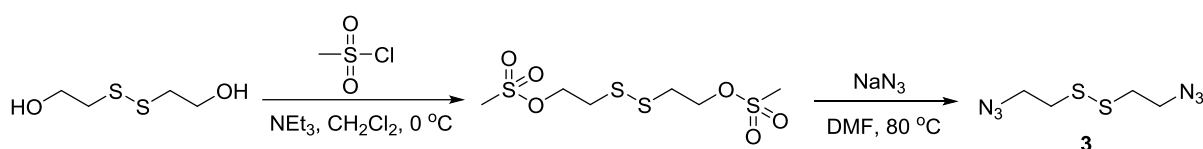
Pyridine (10 eq.) was added to a solution of RAFT CTA-functional polycarbonate, 4-pentynoic anhydride (30 eq.) and DMAP (3 eq.) in dry CH<sub>2</sub>Cl<sub>2</sub> and stirred under nitrogen for 36 h. The solution was washed with saturated NaHSO<sub>4</sub> (2 ×) and saturated NaHCO<sub>3</sub> and the organic layer dried over MgSO<sub>4</sub>. Solvent was removed *in vacuo*, the polymer residue dissolved in the minimum amount of CHCl<sub>3</sub> and precipitated into petroleum ether 40 – 60 °C three times.

**P2<sub>alkyne</sub>:** <sup>1</sup>H NMR (400 MHz, CDCl<sub>3</sub>, ppm):  $\delta$  = 7.31 – 7.26 (m, 4H<sub>backbone-1</sub>, Ar), 5.11 (m, 2H<sub>backbone-1</sub>, OCH<sub>2</sub>Ar), 4.59 (m, 2H<sub>backbone-1</sub>, SCH<sub>2</sub>Ar), 4.28 (m, 8H<sub>backbone-1+2</sub>, C=OOCH<sub>2</sub>C(CH<sub>3</sub>)CH<sub>2</sub>O), 4.17 (m, 2H<sub>backbone-2</sub>, OCH<sub>2</sub>CH<sub>3</sub>), 4.11 (m, 4H<sub>end-group</sub>, OCH<sub>2</sub>CH<sub>2</sub>),

3.87 (m, 2H<sub>backbone-1</sub>, SCH<sub>2</sub>CH<sub>3</sub>), 2.55 (m, 4H<sub>end-group</sub>, CH<sub>2</sub>CH<sub>2</sub>CCH), 2.50 – 2.42 (m, 4H<sub>end-group</sub>, CH<sub>2</sub>CH<sub>2</sub>CCH), 1.97 (m, 2H<sub>end-group</sub>, CH), 1.73 (m, 4H<sub>end-group</sub>, OCH<sub>2</sub>CH<sub>2</sub>), 1.34 (m, 3H<sub>backbone-1</sub>, SCH<sub>2</sub>CH<sub>3</sub>), 1.24 (m, 6H<sub>backbone-1+2</sub>, CCH<sub>3</sub>), 1.22 (m, 3H<sub>backbone-2</sub>, OCH<sub>2</sub>CH<sub>3</sub>).

### Synthesis of bis-(azidoethyl)disulfide (**3**)

**Caution:** Small organic azides are potentially explosive and must be handled with care, particularly in concentrated forms and/or in large quantities. Keep away from sources of temperature, pressure, light, shocks and strong acids.



Bis-(azidoethyl)disulfide (**3**) was prepared according to literature procedures.<sup>4, 5</sup> Methanesulfonyl chloride (4.01 mL, 51.9 mmol) was added dropwise to a solution of 2-hydroxyethyl disulfide (2 g, 13.0 mmol) and triethylamine (7.23 mL, 51.9 mmol) in CH<sub>2</sub>Cl<sub>2</sub> (40 mL) at 0 °C and subsequently left to stir at room temperature for 16 h. The solution was washed with 1M HCl (2 × 20 mL), saturated NaHCO<sub>3</sub> (2 × 20 mL) and brine (20 mL) and the organic layer dried over MgSO<sub>4</sub>. Solvent was removed *in vacuo* to yield bis-(mesyloxyethyl)disulfide as a pale yellow oil, that was used for the next step without further purification.

Sodium azide (4.2 g, 64.6 mmol) was added to a solution of bis-(mesyloxyethyl)disulfide (4 g, 12.9 mmol) in DMF (80 mL) and heated at 80 °C for 16 h, during which time a white precipitate formed. The precipitate was removed *via* filtration and solvent removed *in vacuo*. The residue was dissolved in CH<sub>2</sub>Cl<sub>2</sub>, filtered, washed with saturated NaHCO<sub>3</sub> and the organic layer dried over MgSO<sub>4</sub>. Solvent was removed *in vacuo* to yield **3** as a colourless oil

(2.35 g, 11.5 mmol, 89.2%). Characterization data were in accordance with that previously reported.<sup>4, 5</sup>

**<sup>1</sup>H NMR** (400 MHz, CDCl<sub>3</sub>, ppm):  $\delta$  = 3.59 (t, 4H, N<sub>3</sub>CH<sub>2</sub>, <sup>3</sup>J<sub>H-H</sub> = 6.7 Hz), 2.86 (t, 4H, SCH<sub>2</sub>, <sup>3</sup>J<sub>H-H</sub> = 6.7 Hz). **<sup>13</sup>C NMR** (100 MHz, CDCl<sub>3</sub>, ppm):  $\delta$  = 50.0 (N<sub>3</sub>CH<sub>2</sub>), 37.7 (SCH<sub>2</sub>).

***General procedure for cyclization via the copper-catalyzed azide-alkyne cycloaddition***

A solution of *N,N,N',N'*'-pentamethyldiethylenetriamine (PMDETA) (100 eq.) in toluene (0.05 mM) was bubbled with nitrogen for 1 h. Cu(I)Br (100 eq.) was added and the solution bubbled for a further 30 min. In a separate ampoule a solution of alkyne-terminated RAFT CTA-functional polycarbonate (1 eq.) and **3** (1 eq.) in toluene (1 mM) was degassed *via* 3 freeze-pump-thaw cycles. The degassed solution of polymer and **3** was transferred into a gas-tight glass syringe and added at a rate of 0.3 mL/h to the solution of PMDETA and Cu(I)Br whilst stirred. After complete addition the solution was stirred for a further 3 h, then washed with saturated NaHCO<sub>3</sub> (3 ×) and brine (3 ×) and the organic layer dried over MgSO<sub>4</sub>. Toluene was removed *in vacuo* and the polymer residue was dissolved in CH<sub>2</sub>Cl<sub>2</sub> and stirred in the presence of Cuprisorb beads overnight. The beads were removed *via* filtration and the polymer was precipitated into petroleum ether 40 – 60 °C.

**P<sub>2</sub>cyclic**: **<sup>1</sup>H NMR** (400 MHz, CDCl<sub>3</sub>, ppm):  $\delta$  = 7.31 – 7.25 (m, 4H<sub>backbone-1</sub>, Ar), 5.12 (m, 2H<sub>backbone-1</sub>, OCH<sub>2</sub>Ar), 4.59 (m, 2H<sub>backbone-1</sub>, SCH<sub>2</sub>Ar), 4.28 (m, 8H<sub>backbone-1+2</sub>, C=OOCH<sub>2</sub>C(CH<sub>3</sub>)CH<sub>2</sub>O), 4.17 (m, 2H<sub>backbone-2</sub>, OCH<sub>2</sub>CH<sub>3</sub>), 4.12 (m, 4H<sub>end-group</sub>, OCH<sub>2</sub>CH<sub>2</sub>), 3.37 (m, 2H<sub>backbone-1</sub>, SCH<sub>2</sub>CH<sub>3</sub>), 3.14 – 2.59 (m, 12H<sub>end-group</sub>, CH<sub>2</sub>SSCH<sub>2</sub> + CH<sub>2</sub>CH<sub>2</sub>CCH + CH<sub>2</sub>CH<sub>2</sub>CCH), 1.73 (m, 4H<sub>end-group</sub>, OCH<sub>2</sub>CH<sub>2</sub>), 1.35 (m, 3H<sub>backbone-1</sub>, SCH<sub>2</sub>CH<sub>3</sub>), 1.24 (m, 6H<sub>backbone-1+2</sub>, CCH<sub>3</sub>), 1.22 (m, 3H<sub>backbone-2</sub>, OCH<sub>2</sub>CH<sub>3</sub>).

### General procedure for RAFT polymerizations

The appropriate equivalents of RAFT CTA-functional cyclic or linear polycarbonate, AIBN (0.1 eq. to total RAFT CTA groups) and monomer were loaded into a dry ampoule and dissolved in  $\text{CHCl}_3$ . The reaction mixture was degassed *via* 4 freeze-pump-thaw cycles and refilled with nitrogen. The polymerization was initiated by immersion of the ampoule into an oil bath at 65 °C. After the desired length of time the polymerization was quenched by immersion of the ampoule in liquid nitrogen.

**P4:**  $^1\text{H}$  NMR (400 MHz,  $\text{CDCl}_3$ , ppm):  $\delta$  = 7.22 – 7.15 (m, 4H<sub>PC</sub>, Ar), 5.18 (m, 2H<sub>PC</sub>, SCH<sub>2</sub>Ar), 5.10 (m, 2H<sub>PC</sub>, OCH<sub>2</sub>Ar), 4.27 (m, 8H<sub>PC</sub>, C=OOCH<sub>2</sub>C(CH<sub>3</sub>)CH<sub>2</sub>O), 4.17 (m, 2H<sub>PC</sub>, OCH<sub>2</sub>CH<sub>3</sub>), 3.63 – 3.31 (m, 4H<sub>PNAM</sub>, NCH<sub>2</sub>CH<sub>2</sub>O), 3.37 (m, 2H<sub>PC</sub>, SCH<sub>2</sub>CH<sub>3</sub>), 2.76 – 2.30 (m, 1H<sub>PNAM</sub>, CH<sub>2</sub>CHC=ON(CH<sub>2</sub>)<sub>2</sub>), 1.90 – 1.50 (m, 2H<sub>PNAM</sub>, CH<sub>2</sub>CHC=ON(CH<sub>2</sub>)<sub>2</sub>), 1.36 (m, 6H<sub>PC</sub>, CCH<sub>3</sub>), 1.24 (m, 3H<sub>PC</sub>, OCH<sub>2</sub>CH<sub>3</sub>).

### Characterization Data

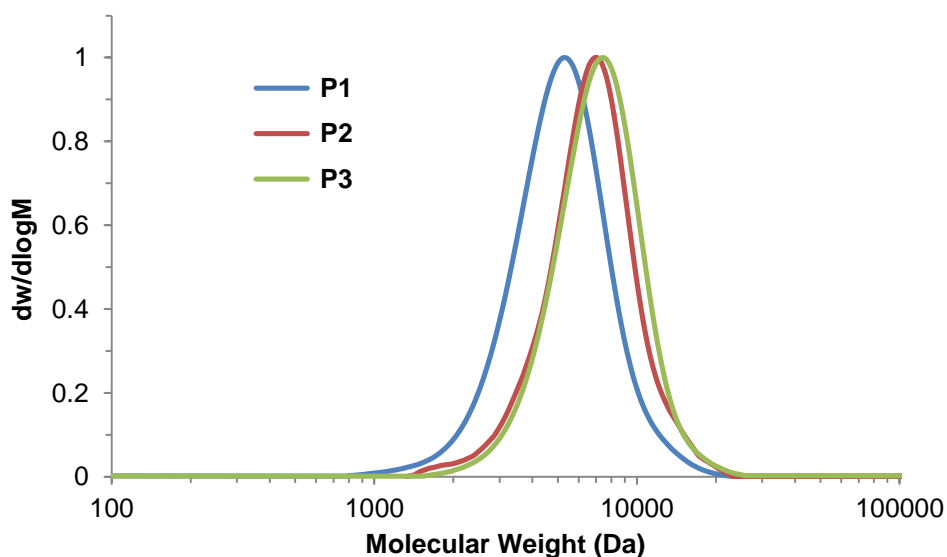


**Figure S1.** Size exclusion chromatograms of polymers **P1** (100% incorporation of **1**,  $M_n$  = 4.6 kDa,  $\mathcal{D}_M$  = 1.21), **P2** (50% incorporation of **1**,  $M_n$  = 6.0 kDa,  $\mathcal{D}_M$  = 1.18) and **P3** (21% incorporation of **1**,  $M_n$  = 6.5 kDa,  $\mathcal{D}_M$  = 1.16) in  $\text{CHCl}_3$  with 0.5%  $\text{NEt}_3$ .



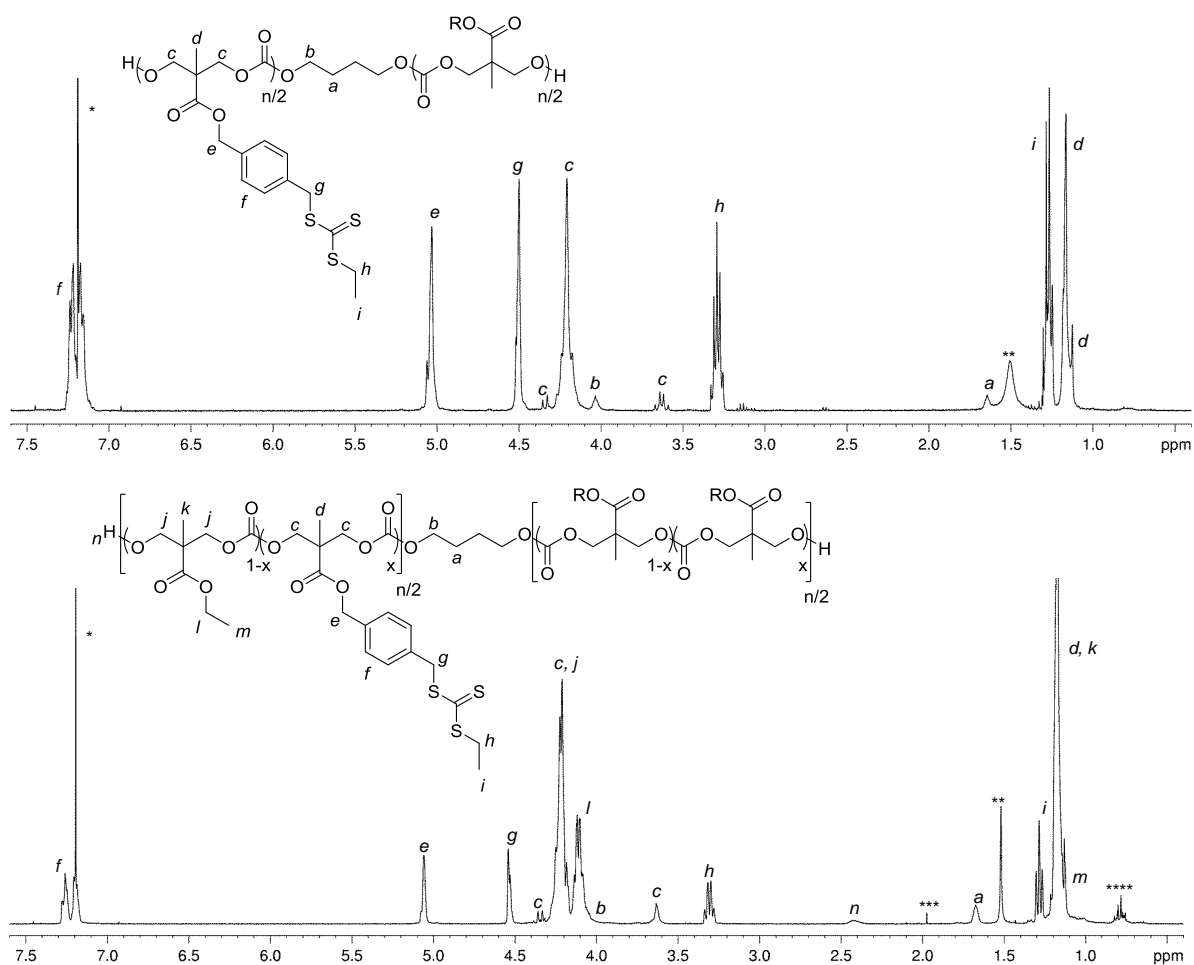


**Figure S2.**  $^1\text{H}$  NMR spectra (400 MHz;  $\text{CDCl}_3$ ) of (top) RAFT CTA-functional polycarbonate homopolymer (**P1**) and (bottom) RAFT CTA- and ethyl-functional polycarbonate copolymer (**P3**) with 21% RAFT CTA functionality (\* $\text{CHCl}_3$ , \*\* $\text{H}_2\text{O}$ , \*\*\*acetone, \*\*\*\*petroleum ether).

**Table S1.** Theoretical and observed  $m/z$  values of **P1**.

DP	Experimental $m/z^a$	Calculated $m/z$
4	1713.3	1713.2
5	2113.4	2113.3
6	2513.5	2513.3
7	2914.6	2913.4
8	3314.7	3313.4

<sup>a</sup>Determined by MALDI-TOF MS analysis using trans-2-[3-(4-*tert*-butylphenyl)-2-methyl-2-propylidene]malonitrile (DCTB) as a matrix, sodium trifluoroacetate as the cationization agent and PEG monomethyl ether 2K standards.

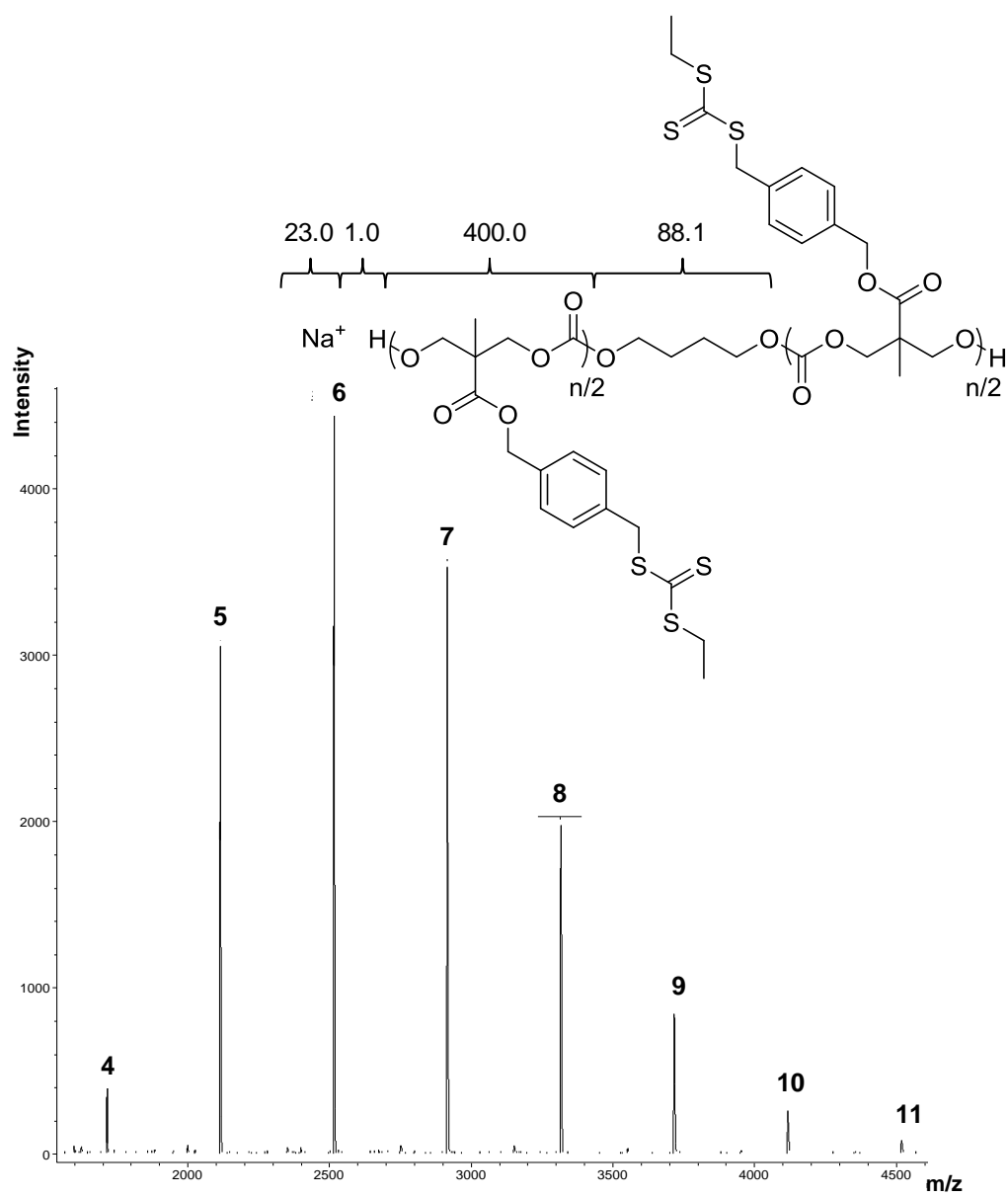


**Figure S3.** MALDI-ToF MS analysis of **P1** (DP = 17) initiated from 1,4-butanediol.

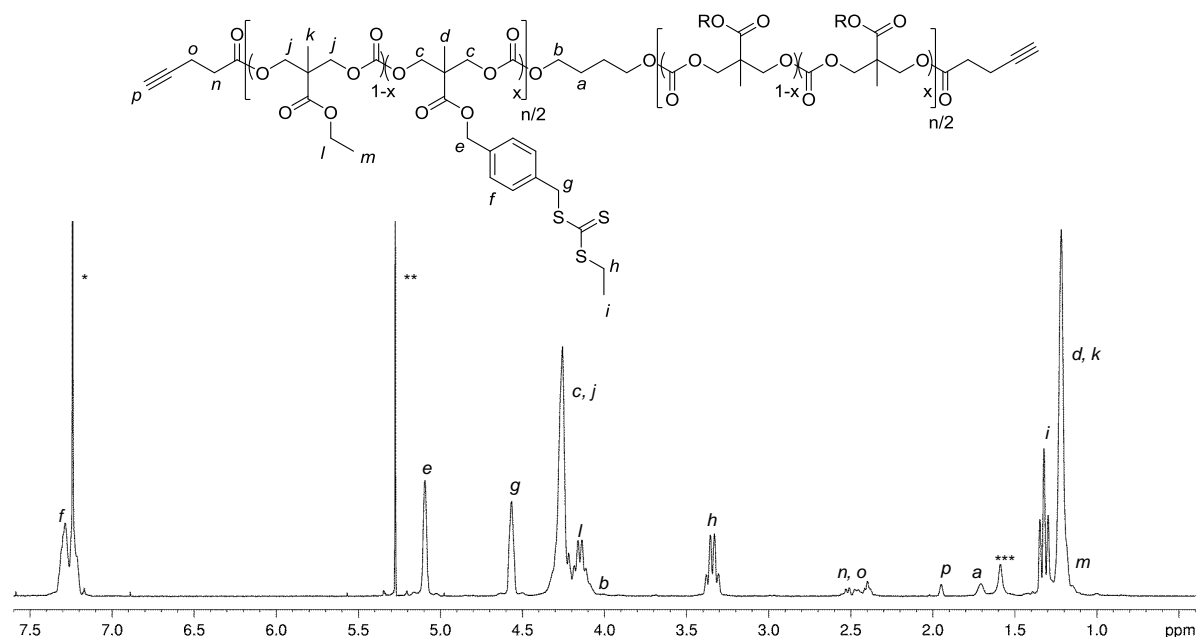


**Figure S4.**  $^1\text{H}$  NMR spectrum (400 MHz;  $\text{CDCl}_3$ ) of alkyne-terminated RAFT CTA-functional polycarbonate copolymer **P2<sub>alkyne</sub>** (\* $\text{CHCl}_3$ , \*\* $\text{CH}_2\text{Cl}_2$ , \*\*\* $\text{H}_2\text{O}$ ).

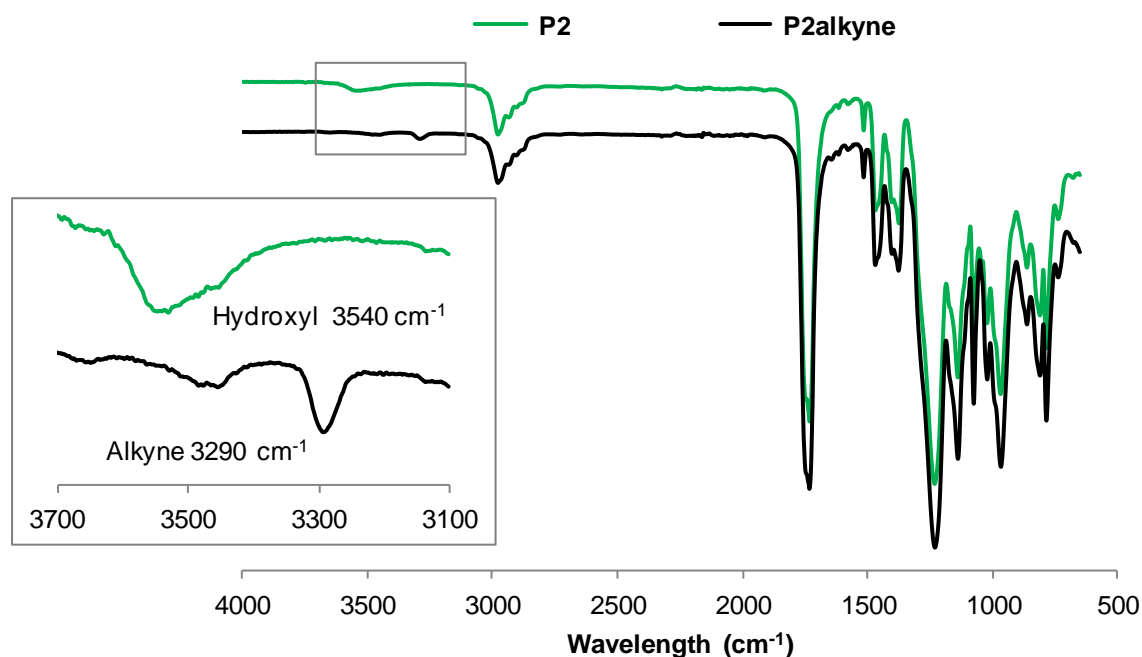


**Figure S5.** FT-IR spectra of hydroxyl-terminated and alkyne-terminated RAFT CTA-functional polycarbonate copolymers **P2** and **P2<sub>alkyne</sub>**. (Inset) Expansion of IR spectra (3700 – 3100  $\text{cm}^{-1}$ ) highlighting peaks that correspond to hydroxyl and alkyne functionalities.

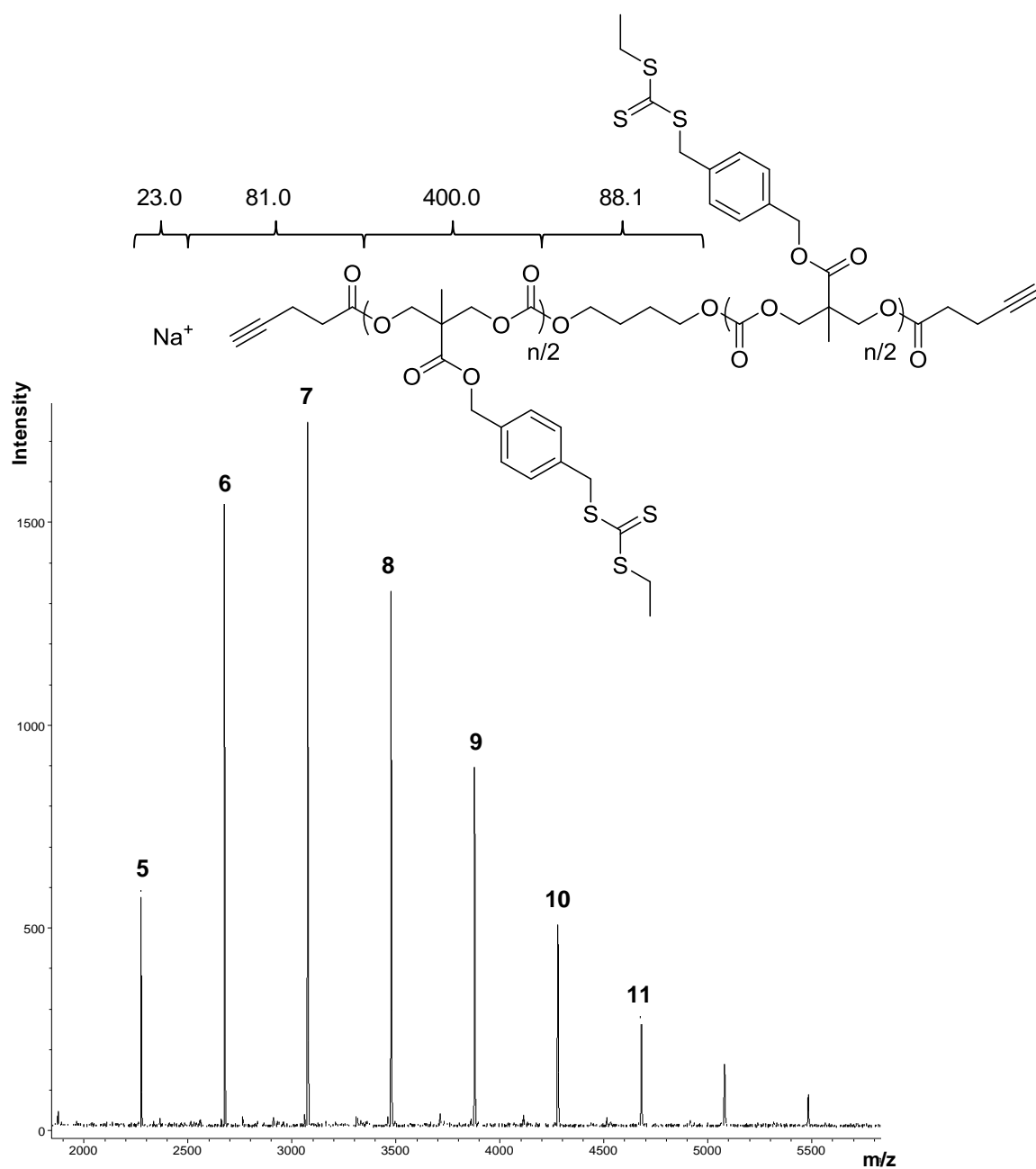


**Figure S6.** MALDI-ToF MS analysis of **P1<sub>alkyne</sub>** (DP = 17) after alkyne end-group functionalization.

**Table S2.** Theoretical and observed  $m/z$  values of alkyne-terminated polycarbonate, **P1**<sub>alkyne</sub>.

DP	Experimental $m/z$ <sup>a</sup>	Calculated $m/z$
5	2273.5	2273.3
6	2673.6	2673.4
7	3073.7	3073.4
8	3473.9	3473.5
9	3874.2	3873.5

<sup>a</sup>Determined by MALDI-TOF MS analysis using trans-2-[3-(4-*tert*-butylphenyl)-2-methyl-2-propylidene]malonitrile (DCTB) as a matrix, sodium trifluoroacetate as the cationization agent and PEG monomethyl ether 2k standards.

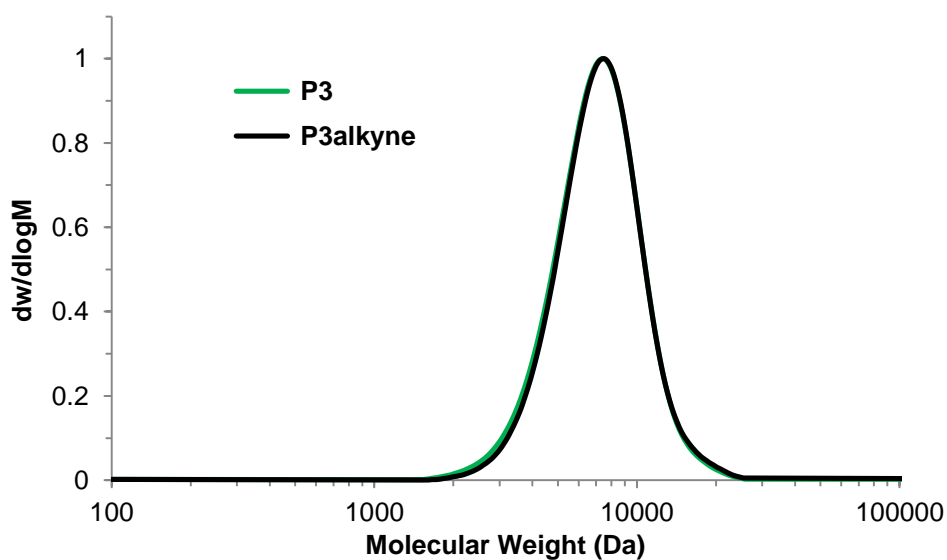


**Figure S7.** Size exclusion chromatograms of hydroxyl-terminated (**P3**,  $M_n = 6.5$  kDa,  $\bar{D}_M = 1.16$ ) and alkyne-terminated (**P3**<sub>alkyne</sub>,  $M_n = 6.7$  kDa,  $\bar{D}_M = 1.15$ ) polycarbonate copolymers in  $\text{CHCl}_3$  with 0.5%  $\text{NEt}_3$ .

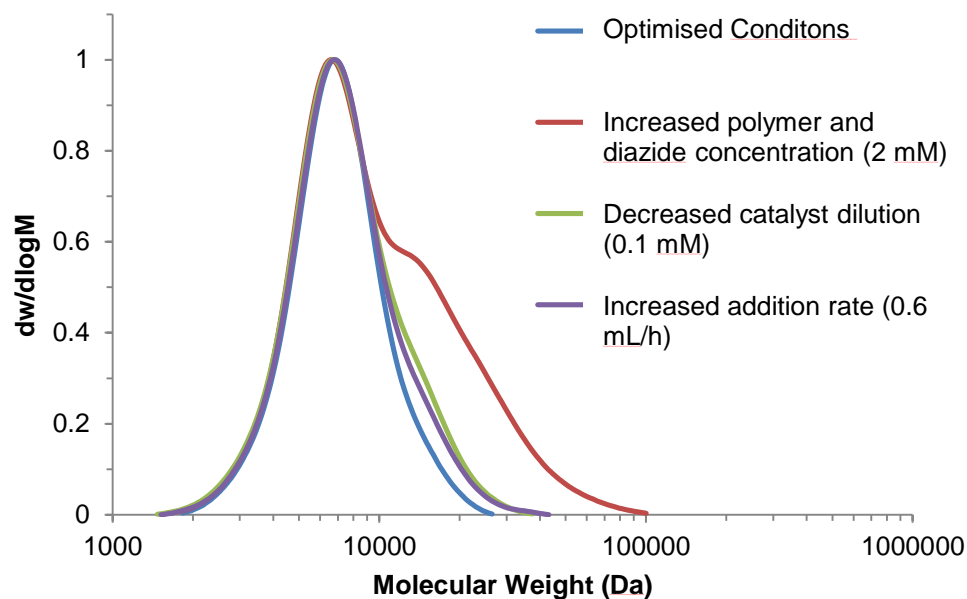


**Figure S8.** Variation of bimolecular cyclization reaction conditions. Size exclusion chromatography performed in  $\text{CHCl}_3$  with 0.5%  $\text{NEt}_3$ .

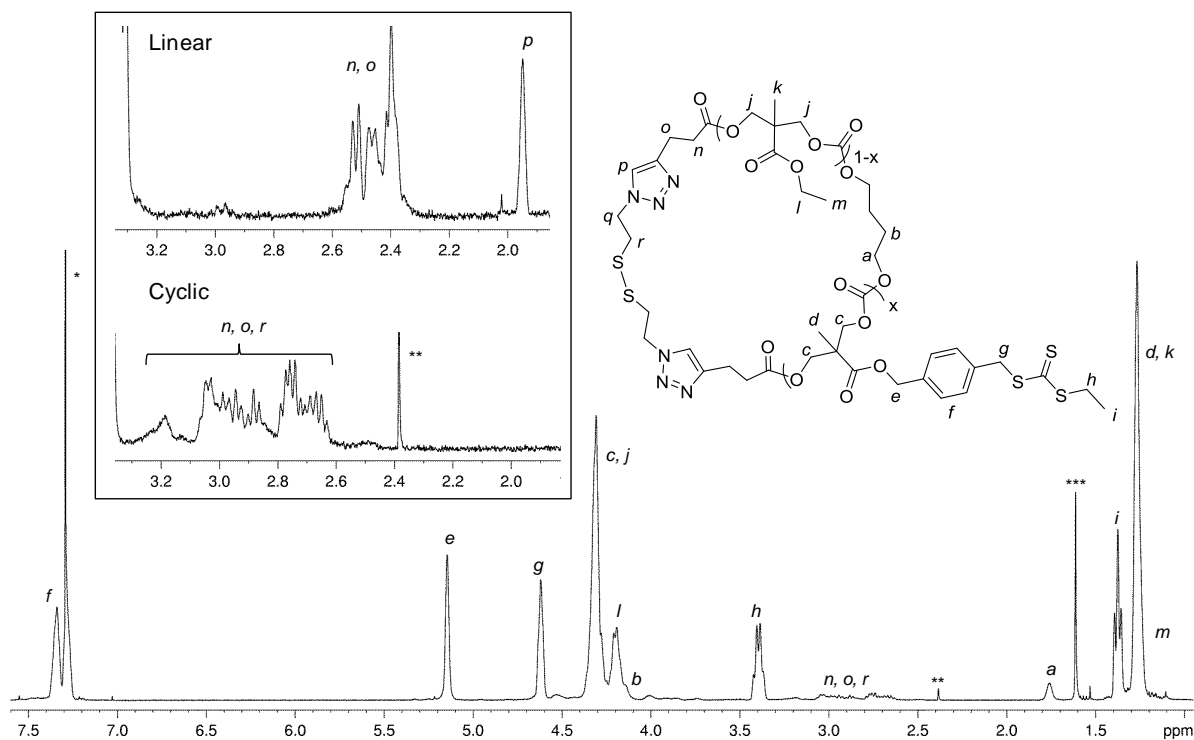


**Figure S9.**  $^1\text{H}$  NMR spectrum (400 MHz;  $\text{CDCl}_3$ ) of cyclized RAFT CTA-functional polycarbonate **P2<sub>cyclic</sub>**. (Inset) Expansion of  $^1\text{H}$  NMR spectra ( $\delta = 3.4 - 1.8$  ppm) of alkyne terminated linear polymer (**P2<sub>alkyne</sub>**) and cyclic polymer (**P2<sub>cyclic</sub>**) (\* $\text{CHCl}_3$ , \*\* toluene, \*\*\* $\text{H}_2\text{O}$ ).

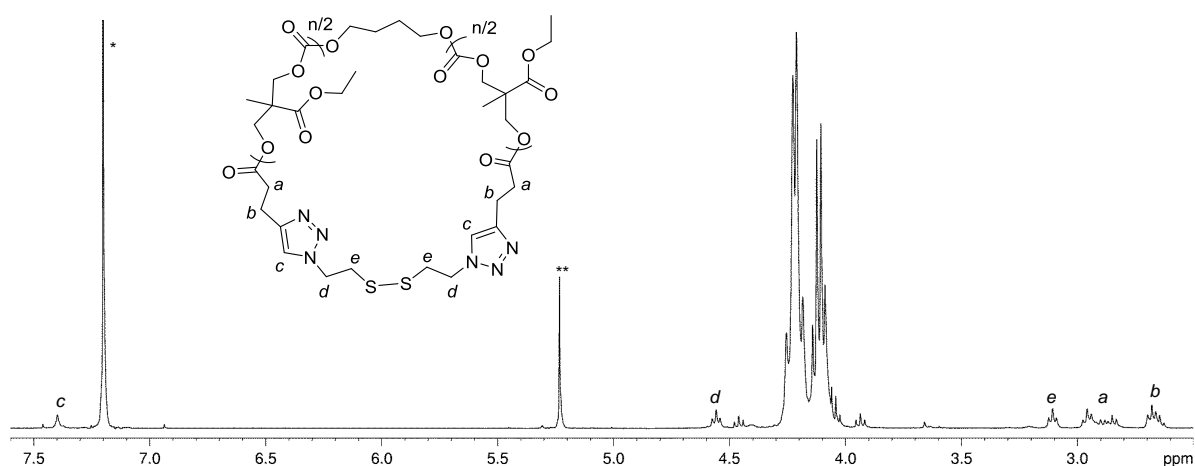


**Figure S10.**  $^1\text{H}$  NMR spectrum (400 MHz;  $\text{CDCl}_3$ ) of cyclized ethyl-functional polycarbonate (\* $\text{CHCl}_3$ , \*\* $\text{CH}_2\text{Cl}_2$ ).

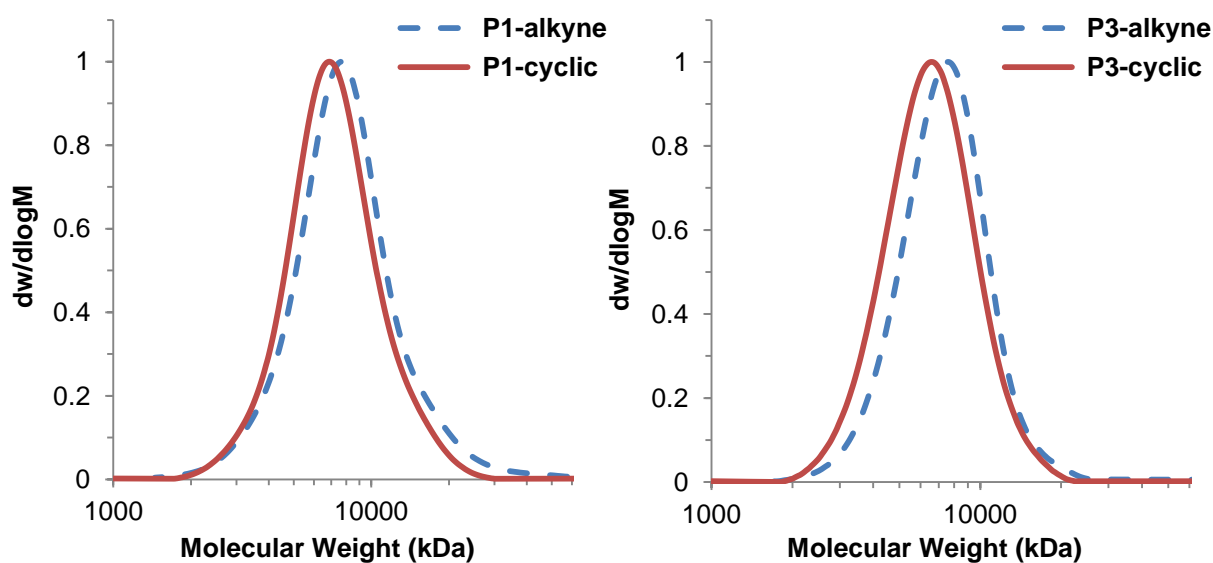
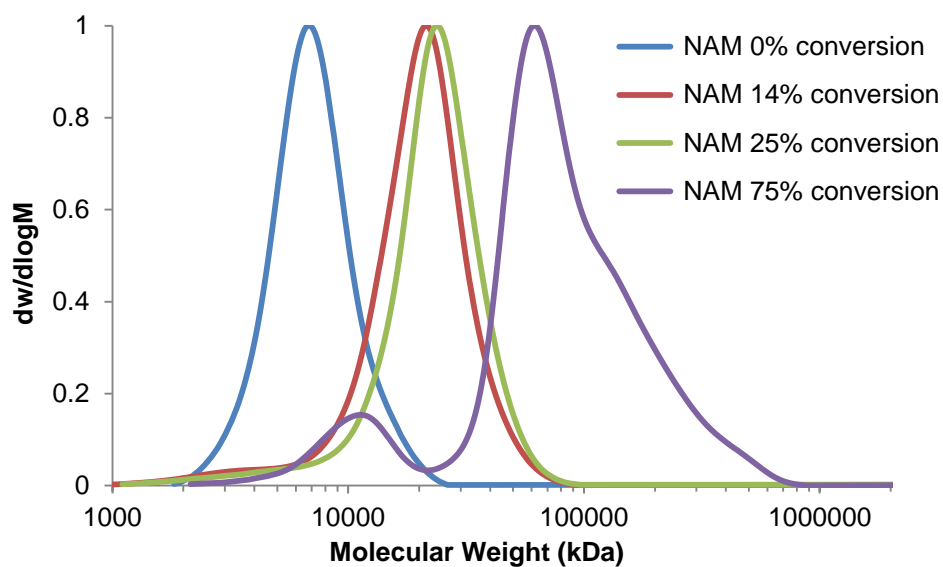


**Figure S11.** Size exclusion chromatograms of RAFT CTA-functional cyclic polycarbonates and alkyne-terminated linear precursor polymers; (left) **P1**<sub>alkyne</sub> ( $M_n = 7.1$  kDa,  $D_M = 1.26$ ) and **P1**<sub>cyclic</sub> ( $M_n = 6.5$  kDa,  $D_M = 1.19$ ), (right) **P3**<sub>alkyne</sub> ( $M_n = 6.7$  kDa,  $D_M = 1.15$ ) and **P3**<sub>cyclic</sub> ( $M_n = 6.0$  kDa,  $D_M = 1.16$ ) in  $\text{CHCl}_3$  with 0.5%  $\text{NEt}_3$ .

**Table S3.** SEC analysis of cyclic polycarbonates, **P1<sub>cyclic</sub>**, **P2<sub>cyclic</sub>** and **P3<sub>cyclic</sub>**.

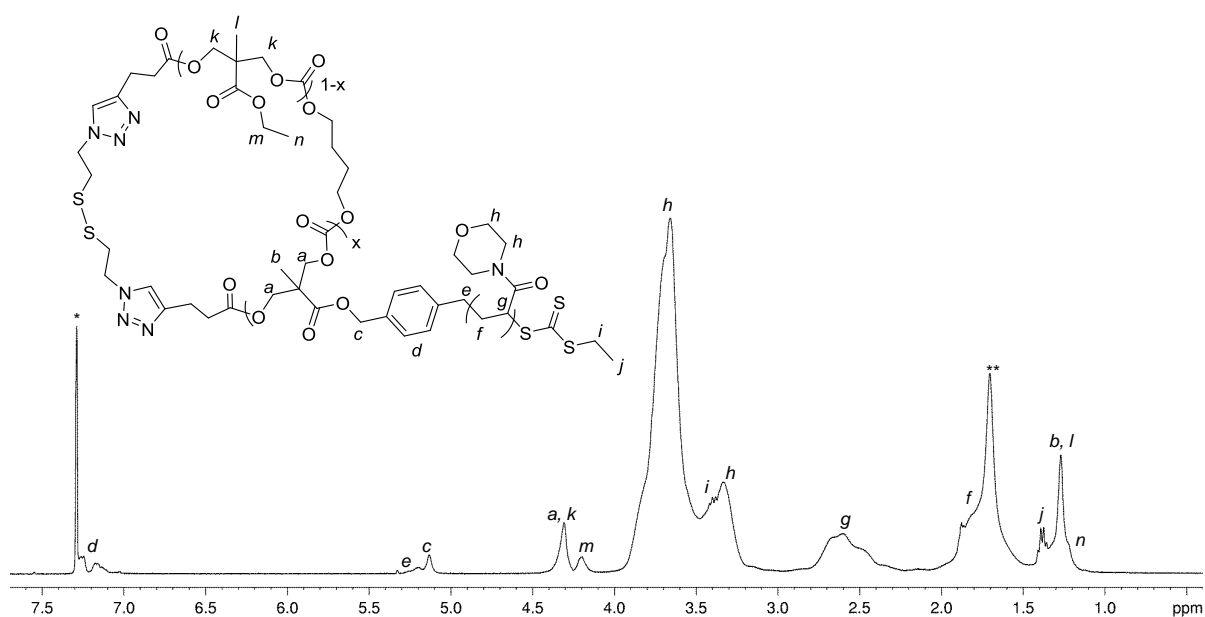
Polymer	$M_n(\text{SEC})_{\text{linear}}$ (kDa) <sup>a</sup>	$\bar{D}_M \text{ linear}^a$	$M_n(\text{SEC})_{\text{cyclic}}$ (kDa) <sup>a</sup>	$\bar{D}_M \text{ cyclic}^a$	$M_n \text{ cyclic} / M_n \text{ linear}^a$
<b>P1<sub>cyclic</sub></b>	7.1	1.26	6.5	1.19	0.9
<b>P2<sub>cyclic</sub></b>	7.4	1.17	6.2	1.16	0.8
<b>P3<sub>cyclic</sub></b>	6.7	1.15	6.0	1.16	0.9

<sup>a</sup>Determined by SEC analysis in CHCl<sub>3</sub> with 0.5% NEt<sub>3</sub> using polystyrene standards.

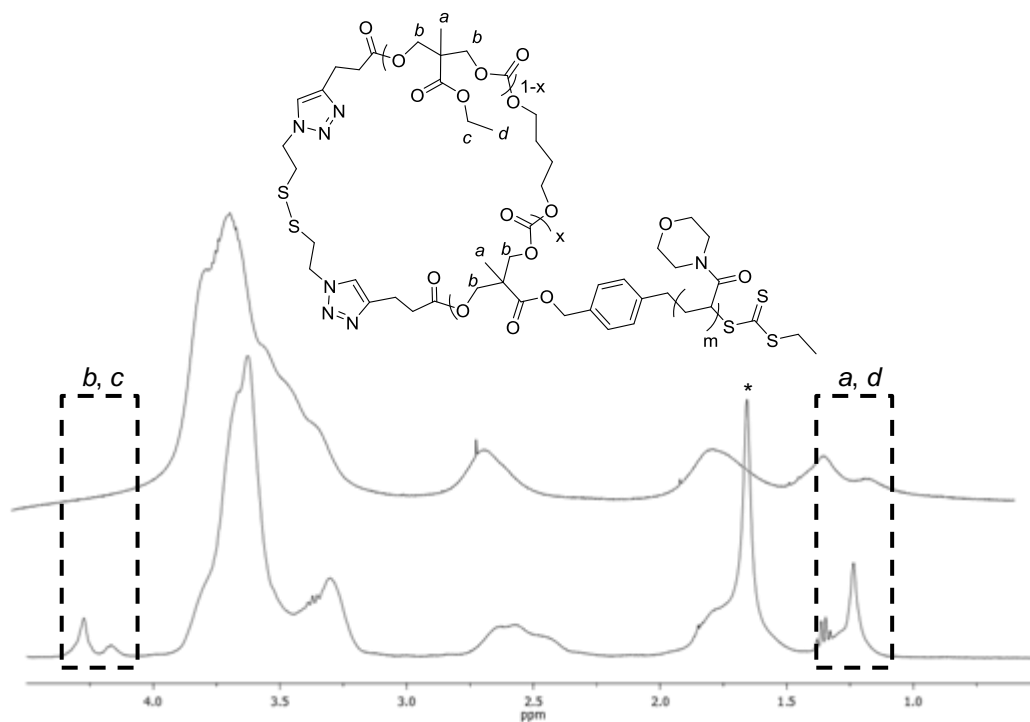


**Figure S12.** Evolution of SEC chromatograms for polymerization of NAM from **P2<sub>cyclic</sub>**. Conditions: [CTA]:[AIBN]:[NAM] = 1:0.1:100, [**P2<sub>cyclic</sub>**] = 0.003 M in CHCl<sub>3</sub> at 65 °C.

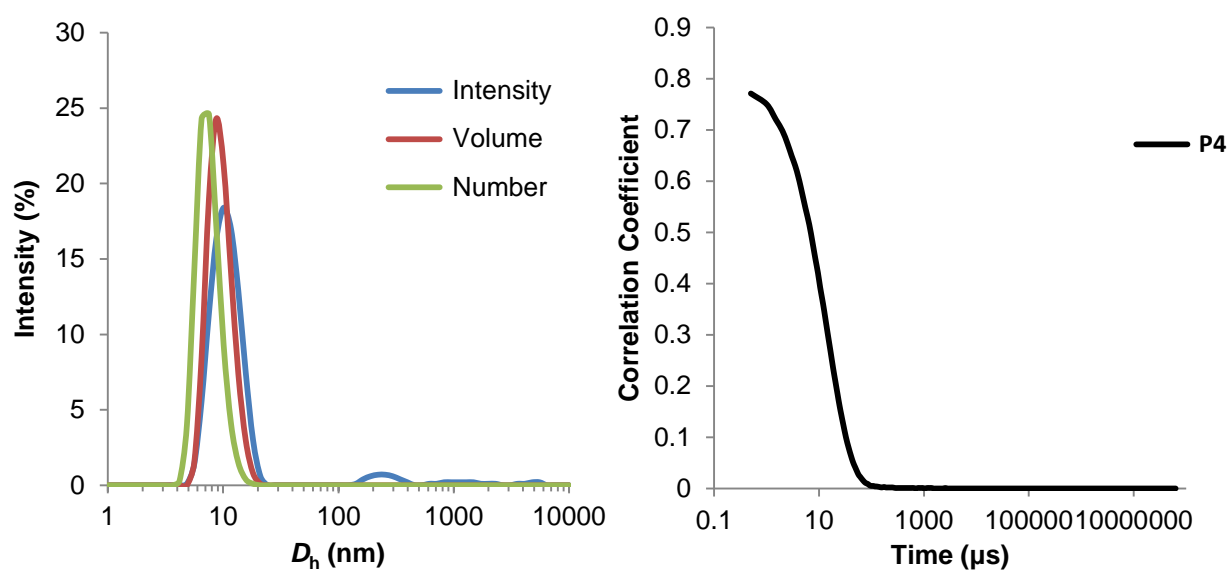




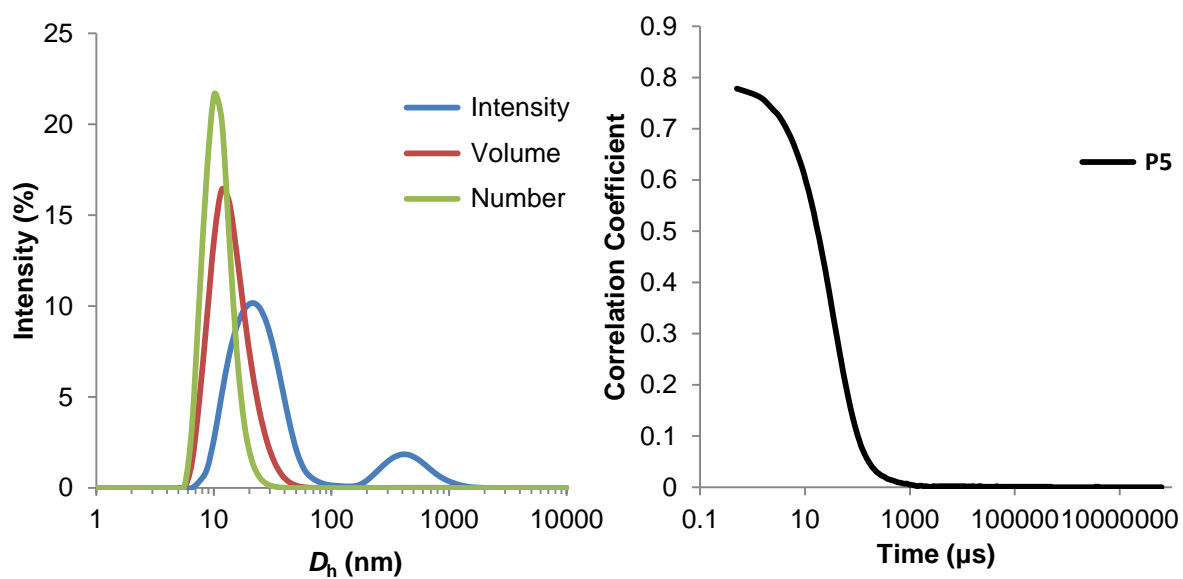
**Figure S13.**  $^1\text{H}$  NMR spectrum (400 MHz;  $\text{CDCl}_3$ ) of *cyclic-polycarbonate-g-poly(NAM)* copolymer **P4** (\* $\text{CHCl}_3$ , \*\* $\text{H}_2\text{O}$ ).



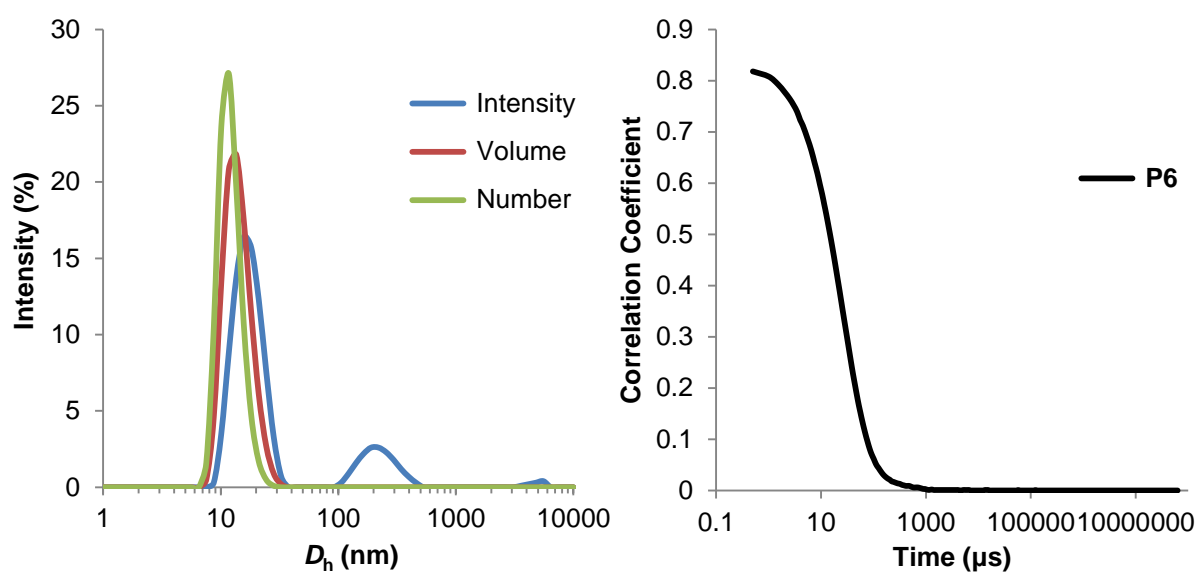
**Figure S14.** Expansion of  $^1\text{H}$  NMR spectra ( $\delta = 4.5 - 0.5$  ppm, 400 MHz) of *cyclic-polycarbonate-g-poly(NAM)* copolymer **P4** in  $\text{CDCl}_3$  (bottom) and  $\text{D}_2\text{O}$  (top) highlighting the attenuation of signals from the polycarbonate backbone in water (\* $\text{H}_2\text{O}$ ).



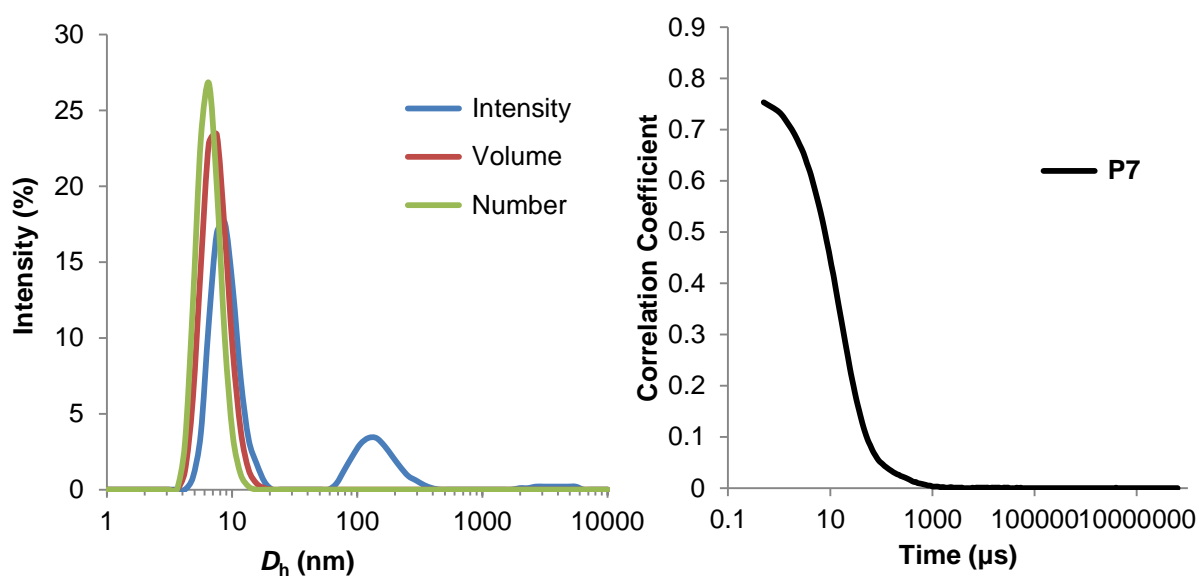
**Figure S15.** DLS analysis of **P4** in 18.2 M $\Omega$ ·cm water; (left) number, volume and intensity profiles, (right) correlation function. PD = 0.193.



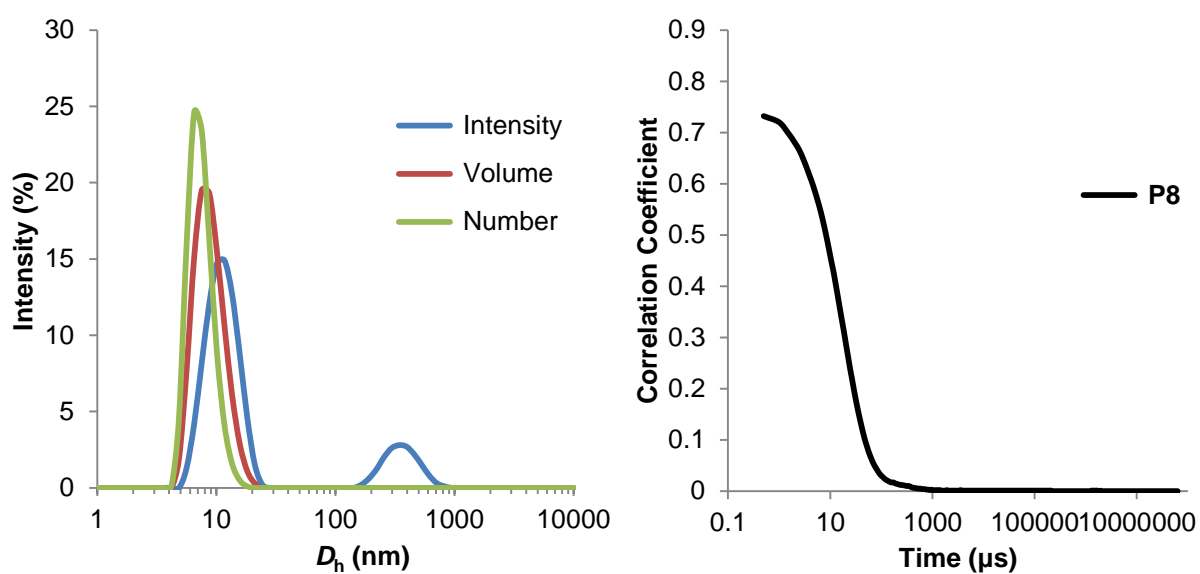
**Figure S16.** DLS analysis of **P5** in 18.2 M $\Omega$ ·cm water; (left) number, volume and intensity profiles, (right) correlation function. PD = 0.307.



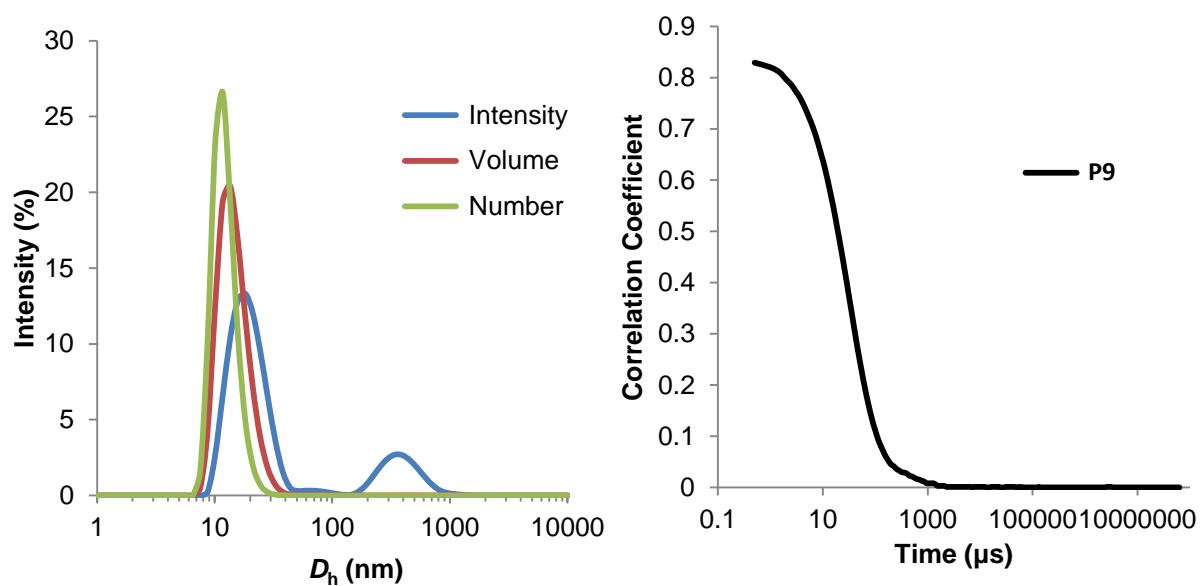
**Figure S17.** DLS analysis of **P6** in 18.2 M $\Omega$ ·cm water; (left) number, volume and intensity profiles, (right) correlation function. PD = 0.274.



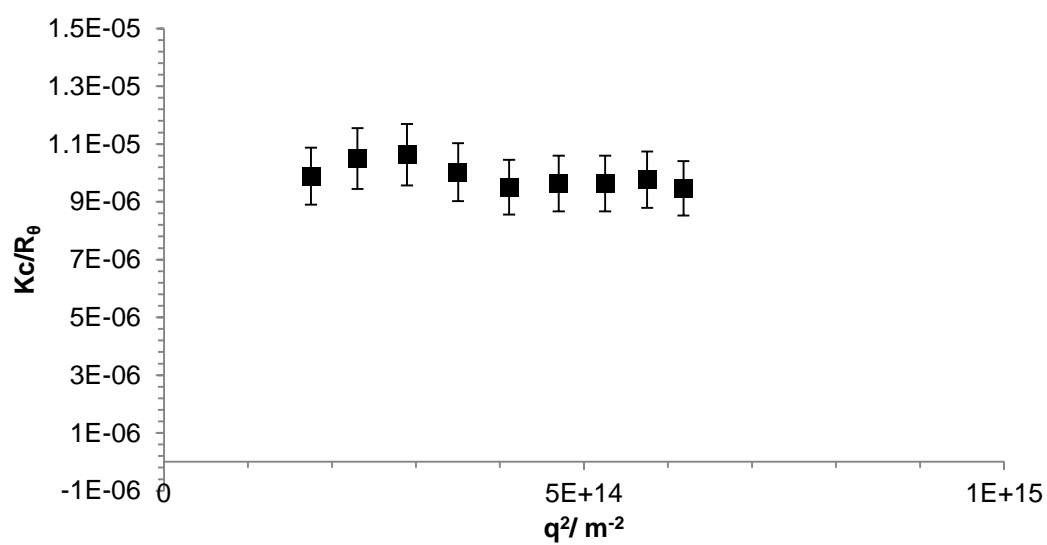
**Figure S18.** DLS analysis of **P7** in 18.2 M $\Omega$ ·cm water; (left) number, volume and intensity profiles, (right) correlation function. PD = 0.364.



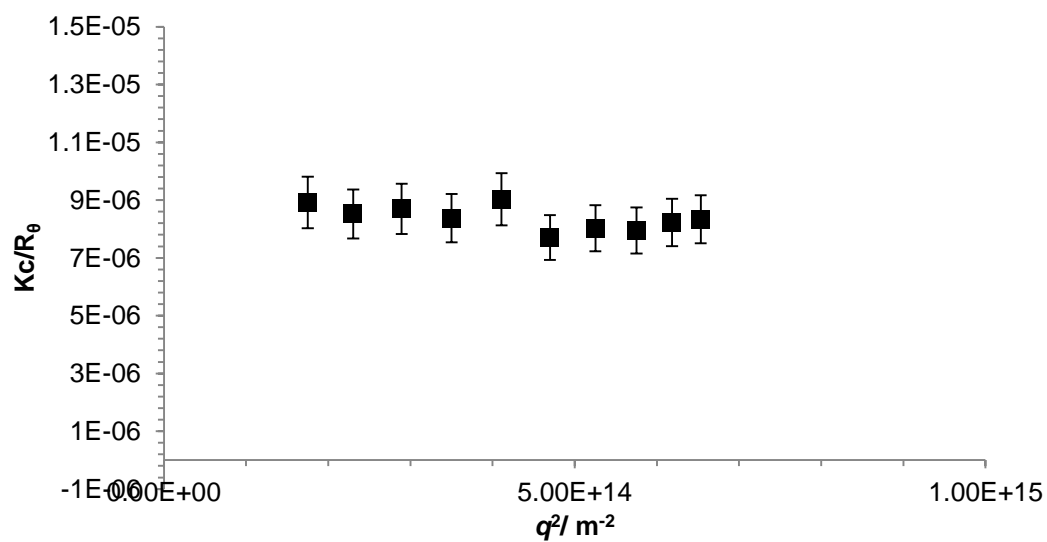
**Figure S19.** DLS analysis of **P8** in 18.2 M $\Omega$ ·cm water; (left) number, volume and intensity profiles, (right) correlation function. PD = 0.306.



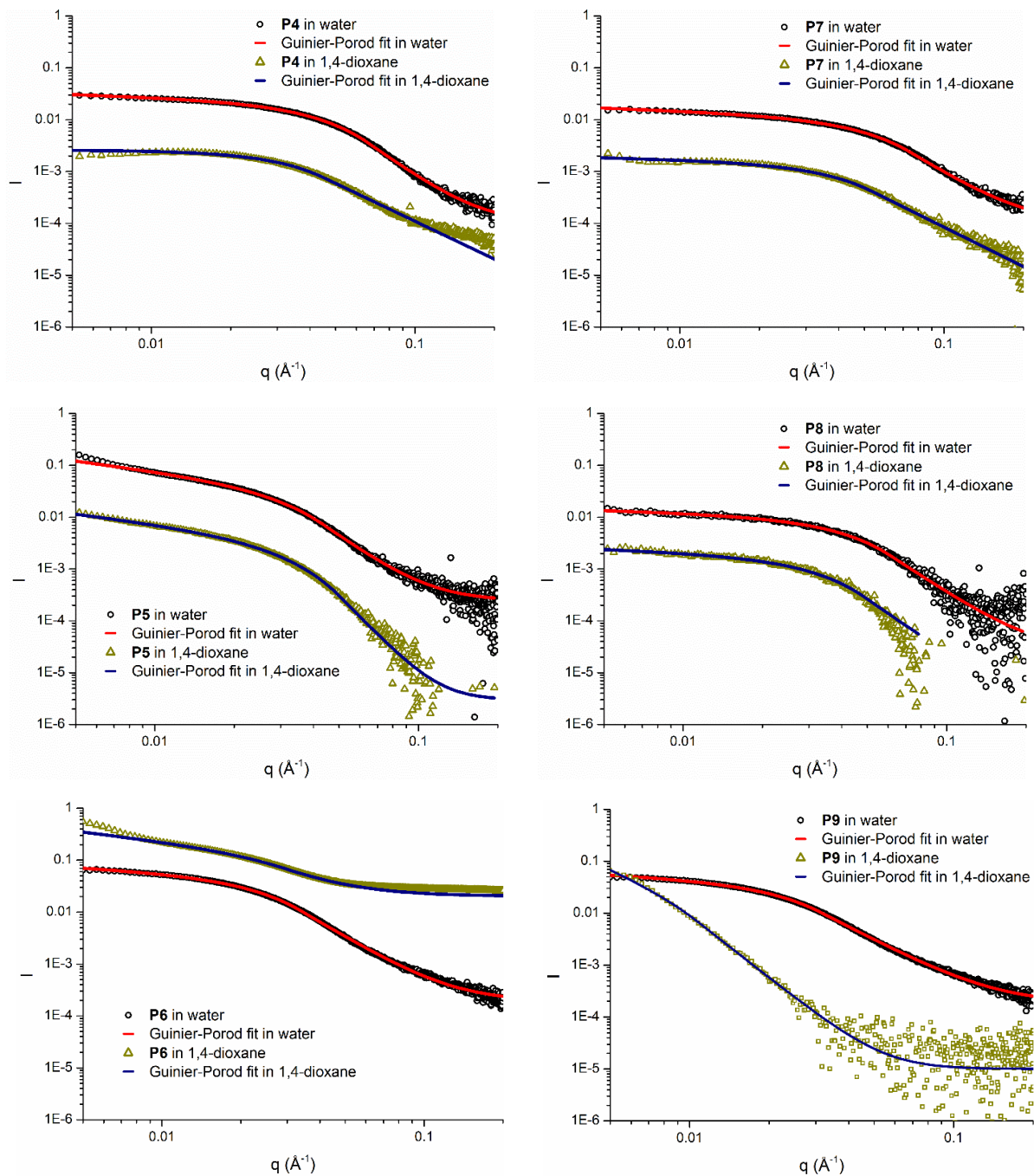
**Figure S20.** DLS analysis of **P9** in 18.2 M $\Omega$ ·cm water; (left) number, volume and intensity profiles, (right) correlation function. PD = 0.328.



**Figure S21.** SLS data plotted as  $Kc/R_\theta$  against  $q^2$  for **P4**



**Figure S22.** SLS data plotted as  $Kc/R_\theta$  against  $q^2$  for **P9**.

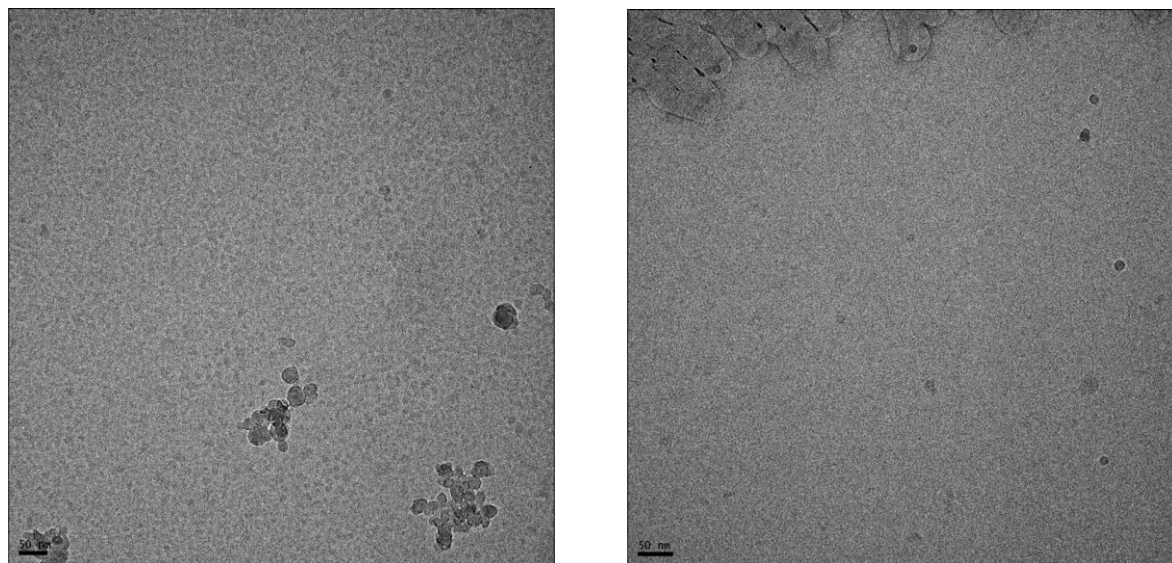


**Figure S23.** SAXS profiles and corresponding Guinier-Porod fits of polymers **P4-P9** in 18.2  $\text{M}\Omega\cdot\text{cm}$  water and 1,4-dioxane. Data in 1,4-dioxane have been shifted vertically by a factor 0.1 for more clarity for the first four graphs.

**Table S4.** AutoRg fit SAXS analysis of cyclic and linear graft copolymers **P4-P9**.

Polymer	PNAM arm length	$R_g(\text{H}_2\text{O})^b$ /nm	$R_g(\text{dioxane})^b$ /nm	$R_g^a/R_h^b$ ( $\text{H}_2\text{O}$ )
<i>cyclic-P4</i>	30	4.1±0.06	4.6±0.07	1.08
<i>linear-P7</i>	30	3.6±0.13	4.1±0.13	1.07
<i>cyclic-P5</i>	50	6.8±0.02 <sup>d</sup>	6.9±0.04 <sup>c</sup>	1.36
<i>linear-P8</i>	50	4.5±0.51	4.4±0.19	1.17
<i>cyclic-P6</i>	110	8.2±0.14	7.71±0.67	1.37
<i>linear-P9</i>	110	7.5±0.72	25.7±2.12 <sup>c, d</sup>	1.15

<sup>a</sup>Determined by SAXS analysis using the AutoRg fit in Primus software, concentration 0.5 mg/mL. <sup>b</sup>Determined by DLS analysis. <sup>c</sup>Aggregation prevented analysis *via* the AutoRg fit, manual Guinier fit performed with Primus in the Tools tab instead. <sup>d</sup>Poor sample collection didn't provide raw data of good quality. Values of  $R_g$  are therefore over-estimated with the manual Guinier fit.

**Figure S24.** CryoTEM images at 2 mg/mL of **P6** (left) and **P9** (right) in 18.2 MΩ·cm water. Scale bar = 50 nm.

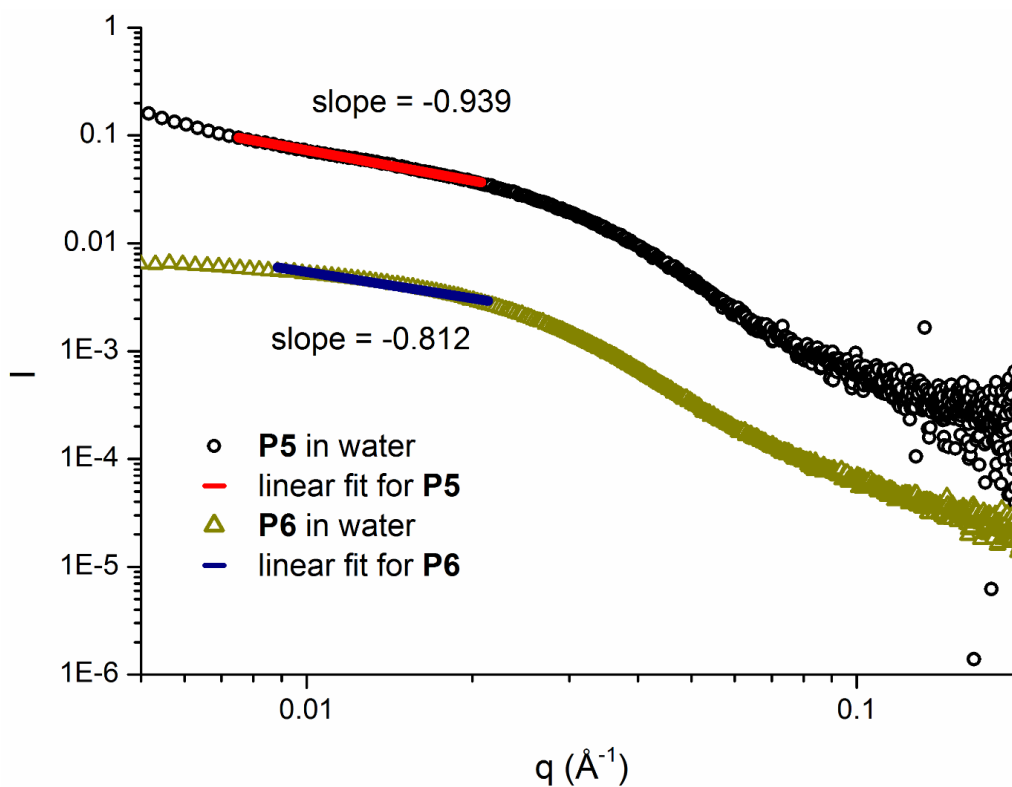


**Figure S25.** Linear fit of the Porod region for **P5** and **P6** in 18.2 MΩ·cm water. All data for **P6** have been shifted vertically by a factor 0.1 for more clarity.

**Table S5.** Characteristics of the linear fit of the Porod region for **P5** and **P6** in 18.2 MΩ·cm water.

	<b>P5</b>	<b>P6</b>
Equation	$y = a \times x + b$	$y = a \times x + b$
$a$	$-0.93892 \pm 0.01354$	$-0.81211 \pm 0.02299$
$b$	$-3.01459 \pm 0.00724$	$-2.88991 \pm 0.04226$
Residual sum of squares	0.00172	0.01001
$R^2$	0.99733	0.96966



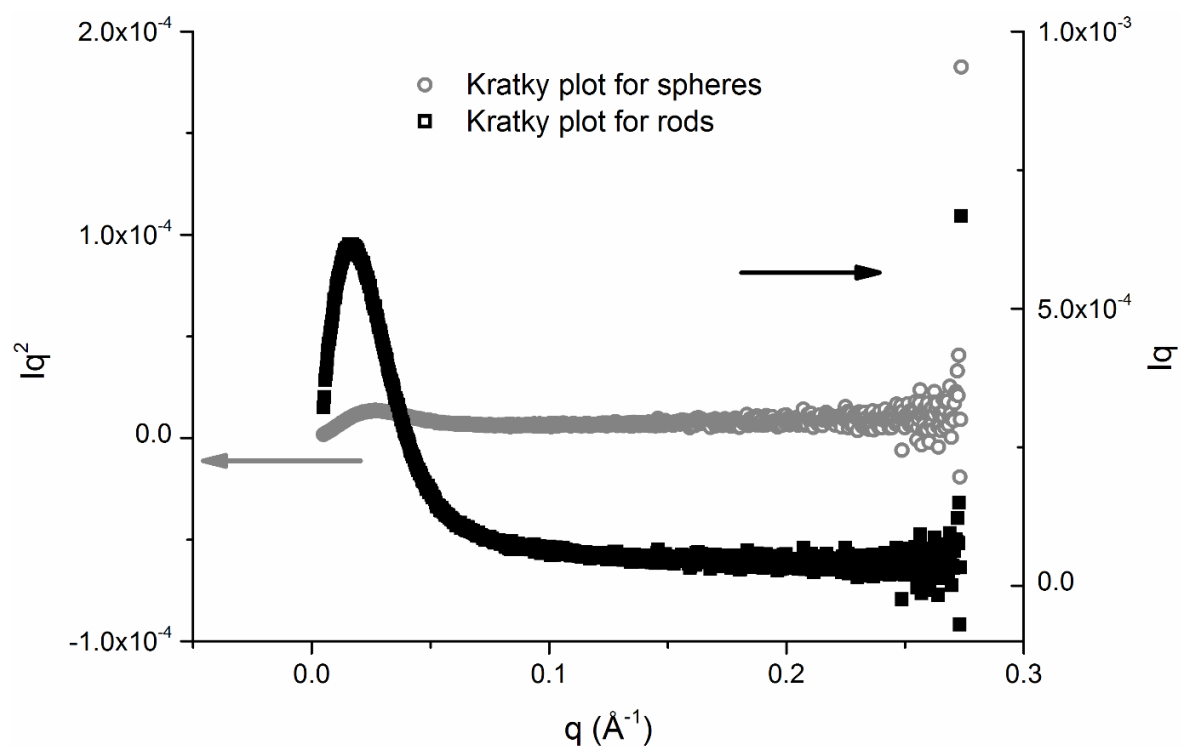


**Figure S26.** Kratky plots for spheres and rods for polymer **P6** in 18.2 MΩ·cm water.

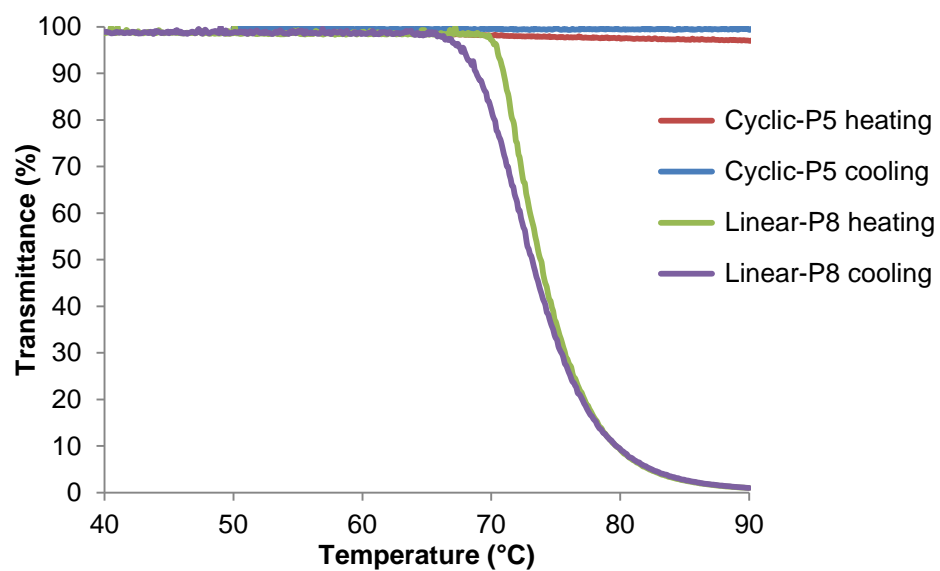


**Figure S27.** Percentage transmittance (%) against temperature (°C) for **P5** and **P8** at 1 mg/mL in 18.2 MΩ·cm water, heating/cooling rate = 1 °C/min.

## References

1. R. J. Williams, R. K. O'Reilly and A. P. Dove, *Polym. Chem.*, 2012, **3**, 2156-2164.
2. K. Fukushima, R. C. Pratt, F. Nederberg, J. P. K. Tan, Y. Y. Yang, R. M. Waymouth and J. L. Hedrick, *Biomacromolecules*, 2008, **9**, 3051-3056.
3. M. Malkoch, K. Schleicher, E. Drockenmuller, C. J. Hawker, T. P. Russell, P. Wu and V. V. Fokin, *Macromolecules*, 2005, **38**, 3663-3678.
4. Y. Wang, R. Zhang, N. Xu, F.-S. Du, Y.-L. Wang, Y.-X. Tan, S.-P. Ji, D.-H. Liang and Z.-C. Li, *Biomacromolecules*, 2010, **12**, 66-74.
5. A. B. J. Withey, G. Chen, T. L. U. Nguyen and M. H. Stenzel, *Biomacromolecules*, 2009, **10**, 3215-3226.